IOPscience iopscience.iop.org

Home Search Collections Journals About Contact us My IOPscience

Experimental evidence for and a projection model of a cubic quasi-crystal

This article has been downloaded from IOPscience. Please scroll down to see the full text article.

1990 J. Phys.: Condens. Matter 2 9749

(http://iopscience.iop.org/0953-8984/2/49/003)

View the table of contents for this issue, or go to the journal homepage for more

Download details:
IP Address: 171.66.16.96
The article was downloaded on 10/05/2010 at 22:45

Please note that terms and conditions apply.

J. Phys.: Condens. Matter 2 (1990) 9749–9755. Printed in the UK

Experimental evidence for and a projection model of a cubic quasi-crystal

Y C Feng†‡, G Lu†‡, H Q Ye†‡, K H Kuo†‡, R L Withers†‡‖ and G Van Tendeloo§

† Laboratory of Atomic Imaging of Solids, Institute of Metal Research, Chinese Academy of Sciences, 110015 Shenyang, People's Republic of China

‡ Beijing Laboratory of Electron Microscopy, Chinese Academy of Sciences, PO Box 2724, 100080 Beijing, People's Republic of China

§ Universiteit Antwerpen, RUCA, Groenenborgerlaan 171, B2020 Antwerp, Belgium

Received 4 June 1990, in final form 10 September 1990

Abstract. A 3D aperiodic structure model with cubic point symmetry is established by projection from a lattice in 6D space. Its Fourier transform describes well the diffraction patterns of the aperiodic phase in rapidly solidified V–Ni–Si and other transition-metal–silicon alloys. This aperiodic phase is suggested to be a quasi-crystal with cubic point group symmetry.

Since the discovery of the icosahedral quasi-crystal in Al–Mn alloys (Shechtman *et al* 1984), quasi-crystals (QCs) with various 2D non-crystallographic point symmetries have been reported, such as the decagonal (Bendersky 1985, Fung *et al* 1986), dodecagonal (Ishimasa *et al* 1985, Chen *et al* 1988) and octagonal (Wang *et al* 1987) phases. These can be described with aperiodic tilings projected from a higher-dimensional cubic lattice. Principally, a QC is not necessarily to be associated with non-crystallographic point group symmetry (Janssen 1988), and it is natural to assume that QCs and corresponding tilings can exist with a crystallographic point symmetry, such as twofold, threefold, fourfold and sixfold rotational symmetry. In fact, electron diffraction patterns (EDPs) consisting of aperiodic Bragg peaks and cubic point symmetry have already been found in rapid solidified $V_6Ni_{16}Si_7$ and other transition-metal–silicon alloys (Feng *et al* 1987, 1989, Lu and Feng 1990). A striking feature of these EDPs is that they have no apparent 'main reflection lattice'. This is essentially different from the conventional incommensurately modulated structures, whose strong diffraction peaks form a periodic lattice surrounded by weak satellite peaks. The absence of the main reflection lattice implies that this aperiodic phase in V–Ni–Si and other related alloys is closer to a QC in diffraction phenomena and may be taken as experimental evidence of the existence of a cubic quasi-crystal (CQC). On the other hand, Kulkarni (1989) generated a 2D quasi-periodic structure with 4 mm point group symmetry. In this paper we construct a model of a QC on the basis of the experimental data in the above transition-metal–silicon alloys, by the cut-and-projection method (Elser 1986). The Fourier transform of this CQC model agrees well with the experimental EDPs.

‖ On leave from Research School of Chemistry, Australia National University, GPO Box 4, Canberra, Australian Capital Territory 2600, Australia.

0953-8984/90/499749 + 07 $03.50 © 1990 IOP Publishing Ltd

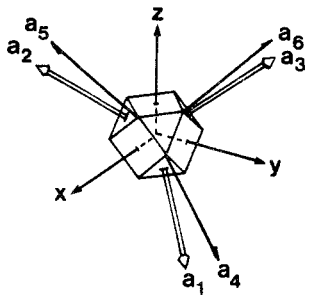

Figure 1. Two sets of basis vectors in 3D physical space used to construct the model.

A close inspection of the EDPs in $V_6Ni_{16}Si_7$ (Feng *et al* 1989) reveals that two sets of reciprocal bases are required to describe the reciprocal structure. These are the bases of a FCC and a BCC lattice respectively, which may be required to have different lattice parameters. From the observation, one may assume a real-space lattice, with cubic point group symmetry, composed of two sets of bonds. One is along $\langle 111\rangle$ directions (type I), and the other along $\langle 110\rangle$ (type II). Only six of the directions are integer independent, as shown in figure 1; hence the rank is 6 (Janssen 1988). A set of bases, $\boldsymbol{a}_i (i = 1, 2, \ldots, 6)$, is chosen as

$$\begin{aligned} \boldsymbol{a}_1 &= \tfrac{1}{2}(11\bar{1}) & \boldsymbol{a}_3 &= \tfrac{1}{2}(\bar{1}11) & \boldsymbol{a}_5 &= (s/2)(101) \\ \boldsymbol{a}_2 &= \tfrac{1}{2}(1\bar{1}1) & \boldsymbol{a}_4 &= (s/2)(110) & \boldsymbol{a}_6 &= (s/2)(011) \end{aligned} \tag{1}$$

where s is a scaling parameter characterizing the length ratio of these two kinds of bond. On this basis, generators of a cubic point group, e.g. 23(T), are represented by

$$\Gamma(2_{\langle 001\rangle}) = \begin{bmatrix} \bar{1} & \bar{1} & \bar{1} & 0 & 0 & 0 \\ 0 & 0 & 1 & 0 & 0 & 0 \\ 0 & 1 & 0 & 0 & 0 & 0 \\ 0 & 0 & 0 & \bar{1} & 0 & 0 \\ 0 & 0 & 0 & \bar{1} & 0 & 1 \\ 0 & 0 & 0 & \bar{1} & 1 & 0 \end{bmatrix} \qquad \Gamma(3_{\langle 111\rangle}) = \begin{bmatrix} 0 & 0 & 1 & 0 & 0 & 0 \\ 1 & 0 & 0 & 0 & 0 & 0 \\ 0 & 1 & 0 & 0 & 0 & 0 \\ 0 & 0 & 0 & 0 & 0 & 1 \\ 0 & 0 & 0 & 1 & 0 & 0 \\ 0 & 0 & 0 & 0 & 1 & 0 \end{bmatrix}.$$

The identity matrix is not given here since it is trivial. It is readily verified that the above matrices are representations of rotation operations $2_{\langle 001\rangle}$ and $3_{\langle 111\rangle}$ by multiplying equation (1) by these matrices. For example, multiplying (1) by matrix $\Gamma(2_{\langle 001\rangle})$ yields a column vector

$$\tfrac{1}{2}\begin{bmatrix} -1 & -1 & -1 \\ -1 & 1 & 1 \\ 1 & -1 & 1 \\ -s & -s & 0 \\ -s & 0 & s \\ 0 & -s & s \end{bmatrix}.$$

This is just equivalent to operate $2_{\langle 001\rangle}$ on (1), resulting in a rotation of π about [001].

Since this 6D matrix representation is 3 + 3 reducible, there exist two 3D orthogonal

subspaces: $E_{\parallel}^3$ and $E_{\perp}^3$. A basis for the representation in the space E^6, written in the components in these two subspaces, is

$$\begin{aligned} \boldsymbol{A}_1 &= (\boldsymbol{a}_1, -c\boldsymbol{a}_1) & \boldsymbol{A}_2 &= (\boldsymbol{a}_2, -c\boldsymbol{a}_2) & \boldsymbol{A}_3 &= (\boldsymbol{a}_3, -c\boldsymbol{a}_3) \\ \boldsymbol{A}_4 &= (\boldsymbol{a}_4, \boldsymbol{a}_4) & \boldsymbol{A}_5 &= (\boldsymbol{a}_5, \boldsymbol{a}_5) & \boldsymbol{A}_6 &= (\boldsymbol{a}_6, \boldsymbol{a}_6) \end{aligned} \tag{2}$$

where $\boldsymbol{A}_1$, for example, has the form $\frac{1}{2}(1, 1, -1, -c, -c, c)$. The short form in equation (2) makes the relationship between the basis vectors in the two 3D subspaces and those in the 6D space clearer. The constant c is the scaling factor in the perpendicular subspace. This basis can be taken as that of a periodic lattice in the 6D space. From the reciprocal relationship, $\boldsymbol{A}_i \times \boldsymbol{A}_j^* = \boldsymbol{\delta}_{ij}$, the reciprocal basis in E^6 is

$$\begin{bmatrix} \boldsymbol{A}_1 \\ \boldsymbol{A}_2 \\ \boldsymbol{A}_3 \\ \boldsymbol{A}_4 \\ \boldsymbol{A}_5 \\ \boldsymbol{A}_6 \end{bmatrix}^* = \frac{1}{1+c} \begin{bmatrix} 1 & 1 & 0 & -1 & -1 & 0 \\ 1 & 0 & 1 & -1 & 0 & -1 \\ 0 & 1 & 1 & 0 & -1 & -1 \\ \frac{c}{s}\begin{bmatrix} 1 & 1 & -1 \\ 1 & -1 & 1 \\ -1 & 1 & 1 \end{bmatrix} & & & \frac{1}{s}\begin{bmatrix} 1 & 1 & -1 \\ 1 & -1 & 1 \\ -1 & 1 & 1 \end{bmatrix} & & \end{bmatrix}. \tag{3}$$

The components of the reciprocal basis vectors $\boldsymbol{A}_i^*$ in the space $E_{\parallel}^3$, i.e. $\boldsymbol{a}_i^*$, are $\langle 110\rangle/(1+c)$ and $\langle 111\rangle c/s(1+c)$. These are two sets of non-equivalent vectors which define two sets of diffraction peaks. As in the cut-and-projection model for an icosahedral QC, the parameter $1/s$ defines the difference in magnitudes of the perpendicular components of the two sets of the reciprocal vectors and thus determines the relative intensities of the two sets of reflections, while the ratio c/s defines the relative positions of them. With proper choice of these parameters, an EDP can be indexed with basis (3). Note that $\boldsymbol{a}_i \times \boldsymbol{a}_j^* \neq \boldsymbol{\delta}_{ij}$ and $\boldsymbol{a}_i$ does not correspond to a set of equally spaced planes and, therefore, corresponds to neither a basis lattice nor a modulated wave.

One notices that the parallel components of the reciprocal basis (3) are just those of BCC and FCC structures. It is then equivalent to rewrite these parallel components in terms of the cubic axes, with BCC and FCC extinction conditions, i.e.

$$\begin{bmatrix} \boldsymbol{b}_1 \\ \boldsymbol{b}_2 \\ \boldsymbol{b}_3 \\ \boldsymbol{b}_4 \\ \boldsymbol{b}_5 \\ \boldsymbol{b}_6 \end{bmatrix}^* = \frac{1}{1+c} \begin{bmatrix} 1 & 0 & 0 & & & \\ 0 & 1 & 0 & & & \\ 0 & 0 & 1 & & & \\ & & & 1 & 0 & 0 \\ & & & 0 & 1 & 0 \\ & & & 0 & 0 & 1 \end{bmatrix} \begin{bmatrix} & & & & & \\ & & & & & \\ & & & & & \\ & & & \frac{c}{s} & & \\ & & & & \frac{c}{s} & \\ & & & & & \frac{c}{s} \end{bmatrix}. \tag{4}$$

With this basis, each diffraction spot can be indexed by six integers (I, J, K, L, M, N) with the constraints $L + M =$ even, $M + N =$ even, $N + L =$ even and $I + J + K =$ even. Basis (4) is more convenient to use in indexing observed diffraction patterns but is less clear in relation to the structure in the hyperspace than is basis (3).

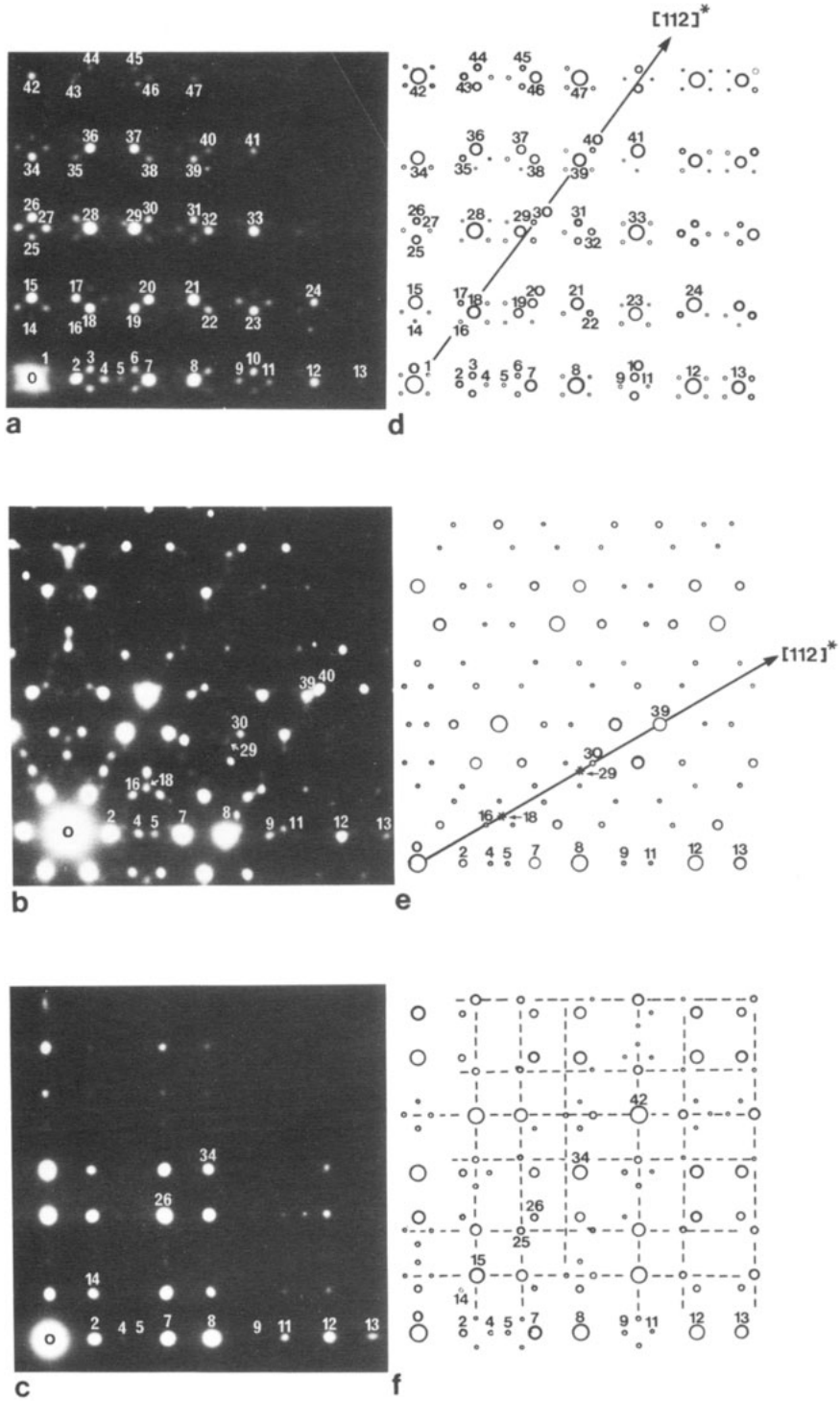

Figure 2. Experimental EDPs from rapidly solidified V–Ni–Si alloy taken along (*a*) ⟨110⟩, (*b*) ⟨111⟩ and (*c*) ⟨001⟩. The corresponding simulated patterns are shown in (*d*), (*e*) and (*f*) for comparison.

Table 1. Indices and amplitudes of some diffraction spots in figure 2(*a*).

Spot	I	J	K	L	M	N		Spot	I	J	K	L	M	N	
0	0	0	0	0	0	0	0.999	26	4	0	0	4	0	0	0.336
1	0	0	0	1	1	1	−0.057	27	4	0	0	3	1	1	0.055
2	0	1	1	0	0	0	0.115	28	4	1	1	3	1	1	0.888
3	0	1	1	1	1	1	0.037	29	4	2	2	3	1	1	0.647
4	0	1	1	0	2	2	0.001	30	4	2	2	4	2	2	0.152
5	0	2	2	0	0	0	−0.001	31	4	3	3	4	2	2	0.294
6	0	2	2	1	1	1	0.187	32	4	3	3	3	3	3	0.282
7	0	2	2	0	2	2	0.609	33	4	4	4	3	3	3	0.997
8	0	3	3	0	2	2	0.913	34	6	0	0	4	0	0	0.831
9	0	4	4	0	2	2	0.079	35	6	1	1	4	0	0	0.240
10	0	4	4	1	3	3	0.362	36	6	1	1	5	1	1	0.674
11	0	4	4	0	4	4	0.032	37	6	2	2	5	1	1	0.475
12	0	5	5	0	4	4	0.863	38	6	2	2	4	2	2	0.491
13	0	6	6	0	4	4	0.684	39	6	3	3	4	2	2	0.755
14	2	0	0	0	0	0	0.003	40	6	3	3	5	3	3	0.181
15	2	0	0	2	0	0	0.788	41	6	4	4	5	3	3	0.763
16	2	1	1	0	0	0	−0.078	42	8	0	0	6	0	0	0.996
17	2	1	1	2	0	0	0.220	43	8	1	1	6	0	0	0.317
18	2	1	1	1	1	1	0.715	44	8	1	1	7	1	1	0.259
19	2	2	2	1	1	1	0.508	45	8	2	2	7	1	1	0.151
20	2	2	2	2	2	2	0.460	46	8	2	2	6	2	2	0.607
21	2	3	3	2	2	2	0.715	47	8	3	3	6	2	2	0.910
22	2	3	3	1	3	3	0.200								
23	2	4	4	1	3	3	0.809								
24	2	5	5	2	4	4	0.673								
25	4	0	0	2	0	0	0.390								

The Fourier transform of the lattice described by (1) is, according to Elser (1986),

$$\varphi = \int \frac{\exp(-i\boldsymbol{x}_\perp \cdot \boldsymbol{q}_\perp)}{V_j} \, d^3x \tag{5}$$

where $q_\perp$ is the component of the reciprocal vector in $E_\perp^3$ and V_j is the volume of the projection window, which is taken as a sphere in 3D space $E_\perp^3$ to the first approximation.

Equations (4) and (5) have been used to calculate the diffraction amplitude of the CQC lattices and to match the experimental diffraction. Various patterns with the CQC characteristic in different alloy systems as in the work of Feng *et al* (1987) can be matched with appropriate choice of parameters c and s. Take rapidly solidified $V_6Ni_{16}Si_7$ alloy as an example, it is found that, with $c/s \simeq 0.6$ and $c \simeq 0.44$, the simulated patterns are in good agreement with the experimental patterns. This is shown in figure 2; figures 2(*a*), 2(*b*) and 2(*c*) are the experimental patterns of ⟨110⟩, ⟨111⟩ and ⟨001⟩ zone axes, respectively, and figures 2(*d*), 2(*e*) and 2(*f*) are the corresponding simulated patterns. For a clear comparison, some important spots in figure 2(*a*) are marked with numbers, and their indices and amplitudes calculated from equation (5) are listed in table 1. The weak reflections arrowed in figure 2(*b*) lie somewhat above or below the {111}* reciprocal plane, such as spots 18 and 29 in figure 2(*d*).

Extinctions occur owing to the symmetry operations in hyperspace (Feng *et al* 1989). On comparison of figures 2(*c*) and 2(*f*), it can be found that the spots on the lines in the calculated pattern (figure 2(*f*)) disappear in the experimental diffraction pattern (figure 2(*c*)). The extinction condition is as follows: $L = 0$, $M + N = 4n + 2$; $M = 0$, $N + L =$

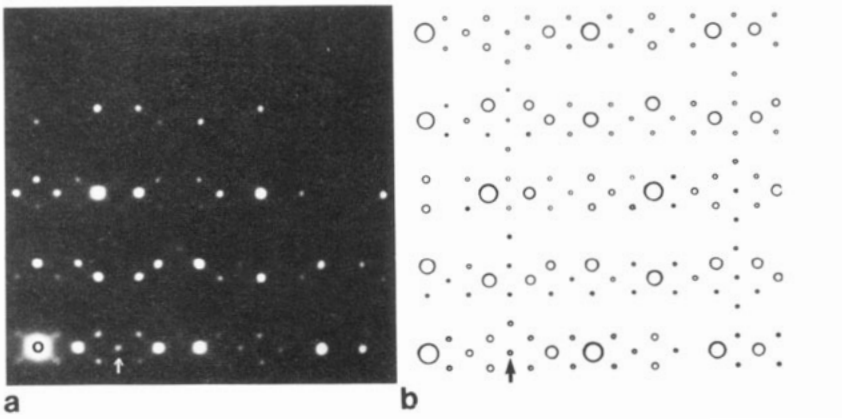

Figure 3. Simulated ⟨110⟩ pattern with $c/s = 1$. The pattern is commensurate. Note that spots 4 and 5 in figure 2 are merged into one, which is arrowed.

$4n + 2$; or $N = 0$, $L + M = 4n + 2$, with n an integer. The extinction rule is very similar to that of the 'diamond' glide plane in a conventional crystal. Note also that some spots in figures 2(a), 2(d) and 2(f), such as spots 15, 25 and 42, disappear in figure 2(c). It has been shown that these spots are actually extinct because of some symmetry operations (Feng *et al* 1989) and their appearance in the experiment (e.g. figure 2(a)) is due to a multiple-diffraction effect (Lu 1989).

The positions and intensities of the diffraction peaks change sensitively with the parameters c and s, while the cubic point group symmetry still remains. As mentioned before, there are two sets of reciprocal basis vectors. For $c/s = 0$, one of them vanishes, leading to a BCC lattice, which corresponds to the γ-brass-like phase (Feng *et al* 1989). When $c/s = \frac{1}{2}$, both sets of bases are active, forming a complicated FCC lattice, as shown in figure 3(b). The corresponding experimental diffraction pattern (figure 3(a)) is found in V–Ni–Si (Feng *et al* 1987). This change in c/s causes many diffraction spots to shift, such as spots 4 and 5 in figures 2(a) and 2(d) move in opposite directions and become one when $c/s = \frac{1}{2}$ as in figure 3. When $0 < c/s < \frac{1}{2}$, a series of COCs can be formed; each has the same point group symmetry but different EDPs, characterized by the relative shift of diffraction spots (Feng *et al* 1987, 1989). For a QC, the spot shift always corresponds to a defect in symmetry, because it has the smallest rank of the point symmetry while, in the COC, the rank of the lattice is 6 and the smallest rank for a lattice of cubic point group is 3, so that the diffraction spots can shift without causing a defect in symmetry. If an icosahedral QC with a rank of 12 is found, it is possible that various diffraction patterns resulting from spot shift with fivefold symmetry should exist.

The above analysis shows that the projected tiling gives Fourier transforms which agree well with the experimental EDPs of the aperiodic phase in rapidly solidified V–Ni–Si and related alloys. This leads us to propose that this phase is a QC with a cubic point group symmetry.

Acknowledgments

This work is supported by the National Natural Science Foundation of China for Youth. The authors are grateful to Professor R H Wang, Professor K K Fung, Professor Q B Yang and Professor Y K Wu for helpful discussions.

References

Bendersky L 1985 *Phys. Rev. Lett.* **55** 1461
Chen H, Li D X and Kuo K H 1988 *Phys. Rev. Lett.* **60** 1645
Elser V 1986 *Acta Crystallogr.* A **42** 36
Feng Y C, Lu G and Withers R L 1989 *J. Phys.: Condens. Matter* **1** 3695
Feng Y C, Zhou D S, Li D X, Dong C, Van Tendeloo G and Kuo K H 1987 *Phil. Mag. Lett.* **55** 221
Fung K K, Yang C Y, Zhou Y Q, Zhan W S and Shen B G 1986 *Phys. Rev. Lett.* **56** 2060
Ishimasa T, Nissen H-U and Fukano Y 1985 *Phys. Rev. Lett.* **55** 511
Janssen T 1988 *Phys. Rep.* **168** 55
Kulkarni U D 1989 *Phys. Rev. Lett.* **63** 2484
Lu G 1989 unpublished work
Lu G and Feng Y C 1991 *Phil. Mag.* at press
Shechtman D, Blech I, Gratias D and Cahn J W 1984 *Phys. Rev. Lett.* **53** 1951
Wang N, Chen H and Kuo K H 1987 *Phys. Rev. Lett.* **59** 1010